Pharm Res (2016) 33:476–486
DOI 10.1007/s11095-015-1803-2

RESEARCH PAPER

Preclinical Pharmacokinetics Evaluation of Anti-heparin-binding EGF-like Growth Factor (HB-EGF) Monoclonal Antibody Using Cynomolgus Monkeys *via* ^{89}Zr-immuno-PET Study and the Determination of Drug Concentrations in Serum and Cerebrospinal Fluid

Noriyuki Kasai [1] • Maiko Adachi [2] • Kazuya Yamano [1]

Received: 23 July 2015 / Accepted: 28 September 2015 / Published online: 13 October 2015

ABSTRACT

Purpose Heparin-binding EGF-like growth factor (HB-EGF) is a member of the EGF family and is an important therapeutic target in some types of human cancers. KHK2866 is a humanized anti-HB-EGF monoclonal antibody IgG that neutralizes HB-EGF activity by inhibiting the binding of HB-EGF to its receptors. The phase I study of KHK2866 was discontinued because of neuropsychiatric toxicity. In this study, the pharmacokinetics of KHK2866 was evaluated by ^{89}Zr-immuno-PET study and the determination of drug concentrations in serum and cerebrospinal fluid using cynomolgus monkeys was performed in order to predict neurotoxicity in a reverse-translational manner.

Methods KHK2866 was radiolabeled with ^{89}Zr for preclinical evaluations in normal cynomolgus monkeys and its distribution was analyzed. Furthermore, as a separate study, KHK2866 concentrations in serum and cerebrospinal fluid were determined after administration of a single dose.

Results PET studies with monkeys revealed ^{89}Zr-KHK2866 accumulation in the liver, spleen and joints of multiple parts, but not in brain. In addition, the pharmacokinetic analyses in serum and CSF demonstrated a low penetration of KHK2866 into the brain.

Conclusions These studies indicate the difficulty of prediction for neuropsychiatric toxicity of monoclonal antibodies in human by means of pharmacokinetic evaluations using cynomolgus monkeys.

KEY WORDS HB-EGF · antibody · ^{89}Zr-immuno-PET · pharmacokinetics

ABBREVIATIONS

BBB	Blood–brain barrier
Bq	Becquerel
CSF	Cerebrospinal fluid
CT	Computed tomography
CTAC	CT-based attenuation correction
EGF	Epidermal growth factor
ELISA	Enzyme-linked immunosorbent assay
FWHM	Full width half maximum
HB-EGF	Heparin-binding EGF-like growth factor
HPLC	High performance liquid chromatography
IACUC	Institutional animal care and use committee
LLOQ	Lower limit of quantification
MIP	Maximum intensity projections
MTD	Maximum tolerated dose
PET	Positron emission tomography
PK	Pharmacokinetics
QC	Quality control
SUV	Standard uptake value
TLC	Thin-layer chromatography
VOI	Volume of interest

Electronic supplementary material The online version of this article (doi:10.1007/s11095-015-1803-2) contains supplementary material, which is available to authorized users.

✉ Noriyuki Kasai
noriyuki.kasai@kyowa-kirin.co.jp

Maiko Adachi
maiko.adachi@kyowa-kirin.co.jp

Kazuya Yamano
kazuya.yamano@kyowa-kirin.co.jp

[1] Singapore Translational Research Laboratory, Kyowa Hakko Kirin (Singapore) Pte. Ltd., 11, Biopolis Way, #05-08, Helios, Singapore 138667

[2] R&D Division, Kyowa Hakko Kirin Co. Ltd., 1188, Shimotogari, Nagaizumi-cho, Sunto-gun, Shizuoka 411-8731, Japan

INTRODUCTION

Epidermal growth factor (EGF) receptors and EGF family members represent promising targets for cancer therapy. Heparin-binding EGF-like growth factor (HB-EGF) is a member of the EGF family and some evidence supports the concept that HB-EGF is a potential therapeutic target in some types of human cancers (1,2).

KHK2866 is a recombinant, humanized, anti-HB-EGF monoclonal antibody (IgG1/κ), which has high affinity (approximately 1 nmol/l) both toward human and monkey HB-EGF. Its parental murine monoclonal antibody, KM3566, exhibits potent *in vivo* anti-tumor activity in murine models *via* direct inactivation of soluble HB-EGF and also immunotherapeutically, *via* antibody-dependent cellular cytotoxicity (ADCC) (3).

The phase Ia study of KHK2866 was conducted to determine the safety, tolerability, maximum tolerated dose (MTD), pharmacokinetics, pharmacodynamics, potential immunogenicity, and preliminary clinical efficacy of KHK2866 administered by intravenous infusion as monotherapy in patients with advanced cancer (4). A phase Ib study was originally planned to determine the MTD of KHK2866 in combination with selected chemotherapies in patients with advanced epithelial ovarian cancer, however, it was not undertaken because of the termination of the phase Ia component (4). In the phase Ia study, grade 2/3 neurotoxicity appeared at doses of 0.1, 1, and 3 mg/kg and it was judged that an adequate safety margin could not be achieved. Neurotoxicity included partial seizure activity, aphasia, and confusion after first-dose administration (4). These effects were reversible, but were not predictable. Toxicology studies performed in cynomolgus monkeys, in which no observed adverse effect level (NOAEL) was ≥100 mg/kg intravenously twice weekly, have not been able to predict human neuropsychiatric adverse effects.

Positron emission tomography (PET) is inherently quite sensitive and enables quantitative imaging at subnanomolar concentrations (5). Furthermore, immuno-PET is a useful tool to assess the distribution of the drug in the whole body and predict its cross-reactivity with normal organs non-invasively. ^{89}Zr is considered to be a suitable isotope because it has a sufficiently long physical half-life (3.3 days) to match the relatively slow pharmacokinetics of an intact antibody. Several ^{89}Zr-immuno-PET studies, for example, using ^{89}Zr-labeled anti-CD44v6 antibody for patients with squamous cell carcinoma of the head and neck (6) and ^{89}Zr-labeled anti-HER2 antibody for breast cancer patients (7) have yielded beneficial information of subjects in clinical trials. Also, preclinical ^{89}Zr-immuno-PET studies of anti-CD44 antibody using cynomolgus monkeys have been reported and have demonstrated the usefulness of immuno-PET imaging to gain better insights into the *in vivo* behavior of the antibody (8).

Taking these studies into account, we conducted two studies using cynomolgus monkeys to predict neurotoxicity from preclinical findings in a reverse-translational manner. First, KHK2866 was radiolabeled with ^{89}Zr and its distribution was analyzed. Second, as a separate study, KHK2866 concentrations in serum and cerebrospinal fluid were determined after administration of a single dose.

MATERIALS AND METHODS

Materials

KHK2866, a full-length recombinant humanized anti-HB-EGF monoclonal antibody (IgG1/κ), was obtained by from Kyowa Hakko Kirin (Tokyo, Japan). KM8047, whose antigen is 2,4-dinitrophenol with the same format (human IgG1/κ), was also obtained from Kyowa Hakko Kirin and used as a control antibody.

Biotin-labeled mouse anti-human IgG monoclonal antibody and ruthenylated monkey anti-human IgG polyclonal antibody were also obtained from Kyowa Hakko Kirin.

Other chemicals and reagents were of the highest grade and purchased from local commercial sources.

Radiolabeling, Quality Control Analyses, and Stability Studies for Immuno-PET Studies

^{89}Zr-N-succinyl-desferrioxamine-KHK2866 and ^{89}Zr-N-succinyl-desferrioxamine-KM8047 were prepared at Vrije Universiteit University Medical Center (Amsterdam, The Netherlands) using previously described methods (9). Radiochemical purity was assessed using TLC and HPLC. Furthermore the stability for a 3-day period was examined to evaluate the stability during shipment to the immuno-PET test site. The antigen-binding activity of ^{89}Zr-KHK2866 was maintained even after the chemical reaction for antibody labeling as the binding activity of cold Zr-N-succinyl-desferrioxamine-KHK2866 prepared in the same manner was confirmed comparable to unlabeled KHK2866 by antigen-coated ELISA (see supplementary Fig. S1).

Immuno-PET Study in Cynomolgus Monkeys

The animal experiments were approved by the Institutional Animal Care and Use Committee (IACUC) of Maccine (Singapore) prior to commencement of the study and conducted at Maccine. In this immuno-PET study, six female, drug naive cynomolgus monkeys, 4–5 years of age and weighing approximately 2–3 kg were used. Animals were fasted for a minimum of 6 h prior to each image acquisition.

The study comprised of two phases. In phase 1, animals (one monkey per group) from the low, medium and high dose

groups got injected with 16.91, 16.64 and 16.06 MBq respectively of the radiolabeled test article ^{89}Zr-KHK2866 *via* slow, intravenous bolus (1–3 min between start and stop of dose administration. Animals from the medium and high dose groups were administered with 1 and 10 mg/kg respectively of the unlabeled antibody KHK2866 also *via* slow, intravenous bolus prior to receiving the radiolabeled test article. The completion of the tracer injection/saline flush was designated as time =0, Day 1 for the determination of nominal sample collection time points and target scan times. All animals underwent whole body PET-CT imaging on Days 1, 4 and 7. On Day 1, the animals were imaged in seated position covering the body in one PET field of view. On Days 4 and 7, the animals were imaged in supine position covering the complete body in four bed positions. Blood samples were taken before tracer injection and 2, 4, 6, 24, 48, 72 and 144 h post tracer injection to measure radioactivity concentrations in whole blood and serum.

In phase 2, animals (one monkey per group) from the low, medium and high dose groups got injected with 15.43, 15.66 and 15.77 MBq respectively of the radiolabeled test article ^{89}Zr-KM8047 *via* slow, intravenous bolus. Animals from the medium and high dose groups were administered with 1 and 10 mg/kg respectively of the unlabeled antibody KM8047 also *via* slow, intravenous bolus prior to receiving the radiolabeled test article. Every scan acquisition and timing of blood sampling was the same as in phase 1.

PET-CT Imaging

Dynamic and static three-dimensional (3D) PET scans were performed using a General Electric Discovery VCT whole body PET-CT scanner (GE Healthcare) with 35 simultaneous slices, axial field of view of 15.7 cm and with an in-plane resolution of 5 mm FWHM.

On Day 1, all animals were placed on the camera bed in seated position. They were subjected to three (3) CT scans (2 scout scans for positioning and 1 CT scan for attenuation correction (CTAC)) prior to the PET scans. The settings for the scout scans were 120 kV and 10 mA and for the CTAC 120 kV and 300 mA, with 0.625 mm slice thickness. An additional reconstruction of 1.25 mm using the Bone Plus kernel was also done. All animals were imaged for 120 min and PET images were acquired in List Mode to allow further re-binning where necessary.

On days 4 and 7, all animals were placed on the camera bed in supine position. They were subjected to three (3) CT scans (2 scout scans for positioning and 1 CT scan for attenuation correction (CTAC)) prior to the PET scans. The settings for the scout scans were 120 kV and 10 mA and for the CTAC 120 kV and 300 mA, with 3.75 mm slice thickness. An additional reconstruction of 0.625 mm using the Bone Plus kernel was also done. All animals were imaged for 120 min and PET images were acquired in non-List Mode.

Data Analysis

Standard uptake values (SUV) were then generated using the following formula:

$$\mathrm{SUV} = \frac{\mathrm{AC_{voi}(kBq/ml)}}{\mathrm{Injected\,dose(MBq)/Body\,weight(kg)}}$$

- AC_{voi} is the average activity concentration, in kBq/ml for each volume of interest (VOI)
- Injected dose is the dose of the tracer administered, in MBq
- Body weight is in kg
- SUV is in g/ml

In total, seven VOIs were processed (brain, heart, left ventricle, left kidney, spleen, liver and left shoulder joint).

Blood Sampling and Processing

Eight whole blood samples of approximately 2 ml were collected from each animal during in-life from the femoral vessels *via* direct venipuncture. A small aliquot of ~100 µl blood was transferred into pre-weighed tubes before the rest of the blood sample was carefully transferred into serum separator tubes and incubated at room temperature for 30 min (max 2 h). Time points of sampling include pre-dose, 2, 4, 6, 24, 48, 72, and 144 h after tracer injection. Serum separator tubes were centrifuged for 10 min at 2500 g to obtain serum. A small aliquot of ~100 µl serum was transferred into pre-weighed tubes. Both set of tubes (whole blood and serum) were weighed again to obtain the net sample weights. Both whole blood and serum aliquots were analyzed in a dedicated PET gamma counter (2480 Wizard2, Perkin Elmer) normalized to measure ^{89}Zr and cross-calibrated with the PET camera. Measured activity was decayed, corrected to time of injection, and expressed as SUV.

PK Analysis

Serum concentrations of decayed ^{89}Zr-KHK2866 and ^{89}Zr-KM8047 were measured by an electrochemiluminescence assay as described below for the determination of human IgG in monkey serum. One serum sample obtained prior to dosing and seven serum samples obtained approximately 2, 4, 6, 24, 48, 72 and 144 h post dosing were used to measure the concentrations.

Pharmacokinetic parameters for individual animal were obtained by non-compartmental analysis (Bolus intravenous administration model) using Phoenix WinNonlin (Pharsight Corporation). The slope of the elimination phase (λz) was calculated using the concentrations of the last three sampling points.

Determination of Serum Concentrations of Decayed ^{89}Zr-KHK2866 and ^{89}Zr-KM8047 by an Electrochemiluminescence Assay

Biotin-labeled mouse anti-human IgG monoclonal antibody as a capture antibody (1 μg/ml in PBS containing 1 w/v% casein) was added to the wells of the microtiter plate, MULTI-ARRAY 96-well Streptavidin Gold Plate (Meso Scale Discovery, catalogue number L15SA), and then incubated for 1 h at room temperature. The wells were washed three times with wash buffer (PBS containing 0.05% Tween 20) and 51-fold diluted calibration standards and analytical samples (diluent: PBS containing 1 w/v% casein) were added to each well of the plate and incubated for 2 h at room temperature. The plate was washed three times, followed by addition of detection antibody (ruthenylated monkey anti-human IgG polyclonal antibody, 0.25 μg/ml in PBS containing 1 w/v% casein). After incubation for 1 h at room temperature, the plate was washed three times. Thereafter, Read Buffer T with Surfactant (Meso Scale Discovery, catalogue number R92TC-1) was added to each well and electrochemiluminescent signals were detected using SECTOR® Imager 2400 (Meso Scale Discovery).

The LLOQ was set to be 100 ng/ml. A calibration curve was generated by 4-parameter regression of the natural logarithmic transformed nominal concentrations of the calibration standards (X axis), except for the 0 μg/ml sample, and the natural logarithmic transformed mean values of duplicate signal intensity (Y axis) using SOFTmax® PRO (Molecular Devices Japan). ^{89}Zr-KHK2866 or ^{89}Zr-KM8047 concentrations were calculated by substitution of the signal intensity to the regression equation of each calibration curve. The validation data of the assay method and calibration curves generated in the validation are shown in supplementary Table S1-2 and Fig. S2, respectively.

Evaluation of Serum and CSF Pharmacokinetics Following a Single Intravenous Dose of KHK2866 and KM8047 in Cynomolgus Monkeys

The animal experiments were approved by the IACUC of Maccine (Singapore) prior to commencement of the study and conducted at Maccine.

In this PK study, 12 female, drug naive cynomolgus monkeys, 3–5 years of age and weighing approximately 2–3 kg were used. Prior to dosing, monkeys were surgically prepared with indwelling cannulae inserted into the cisterna magna and connected to a subcutaneous access port to permit CSF sampling. Animals were randomly assigned to six dose groups. For KHK2866, animals were administered with 1, 10, and 100 mg/kg (two monkeys per group) *via* slow, intravenous bolus. Similarly, for KM8047 (control antibody), animals were administered with 1, 10, and 100 mg/kg (two monkeys per group) *via* slow, intravenous bolus. CSF and serum samples were obtained at multiple time points; pre-dose, 1, 3, 6, 24, 48, 96, and 168 h post dose. Concentrations of KHK2866 and KM8047 in serum and CSF were determined using an electrochemiluminescence assay by the same method described above with minor modification. The LLOQ was set to be 100 ng/ml and 5 ng/ml for serum and CSF samples, respectively.

Pharmacokinetic parameters for individual animal were obtained by non-compartmental analysis (Bolus intravenous administration model for serum, Extravascular administration model for CSF) using Phoenix WinNonlin (Pharsight Corporation). The slope of the elimination phase (λz) was calculated using the concentrations of the last three sampling points, however, when the model did not converge, the next last three points were used for the analysis removing the last one point.

RESULTS

Radiolabeling, Quality Control Analyses, and Stability Studies

QC tests for ^{89}Zr-N-succinyl-desferrioxamine-KHK2866 and ^{89}Zr-N-succinyl-desferrioxamine-KM8047 were performed at the end of synthesis and again, at 2 or 3 days after the end of synthesis. Both tracer productions showed 100% radiochemical purity on all days measured by HPLC and greater than 98% radiochemical purity when measured using TLC.

Immuno-PET Study in Cynomolgus Monkeys

PET-CT Imaging of ^{89}Zr-N-succinyl-desferrioxamine-KHK2866

All animals underwent whole body PET-CT imaging on Days 1, 4 and 7. In general, the biodistribution of ^{89}Zr-KHK2866 was similar for the 3 doses (0.1, 1 and 10 mg/kg) (Figs. 1a and 2a-c). The maximum intensity projections (MIP) showed that ^{89}Zr-KHK2866 remained in the systemic circulation well after 2 h (data not shown) and accumulated in the liver, spleen and joints of multiple parts including mandibular, knees, shoulders, elbows, and wrists. The kinetic analysis for ^{89}Zr-KHK2866 demonstrated a poor penetration into the brain, and a wash-out from the circulation which went well beyond 7 days post-injection. The heart, kidneys and liver elicited the

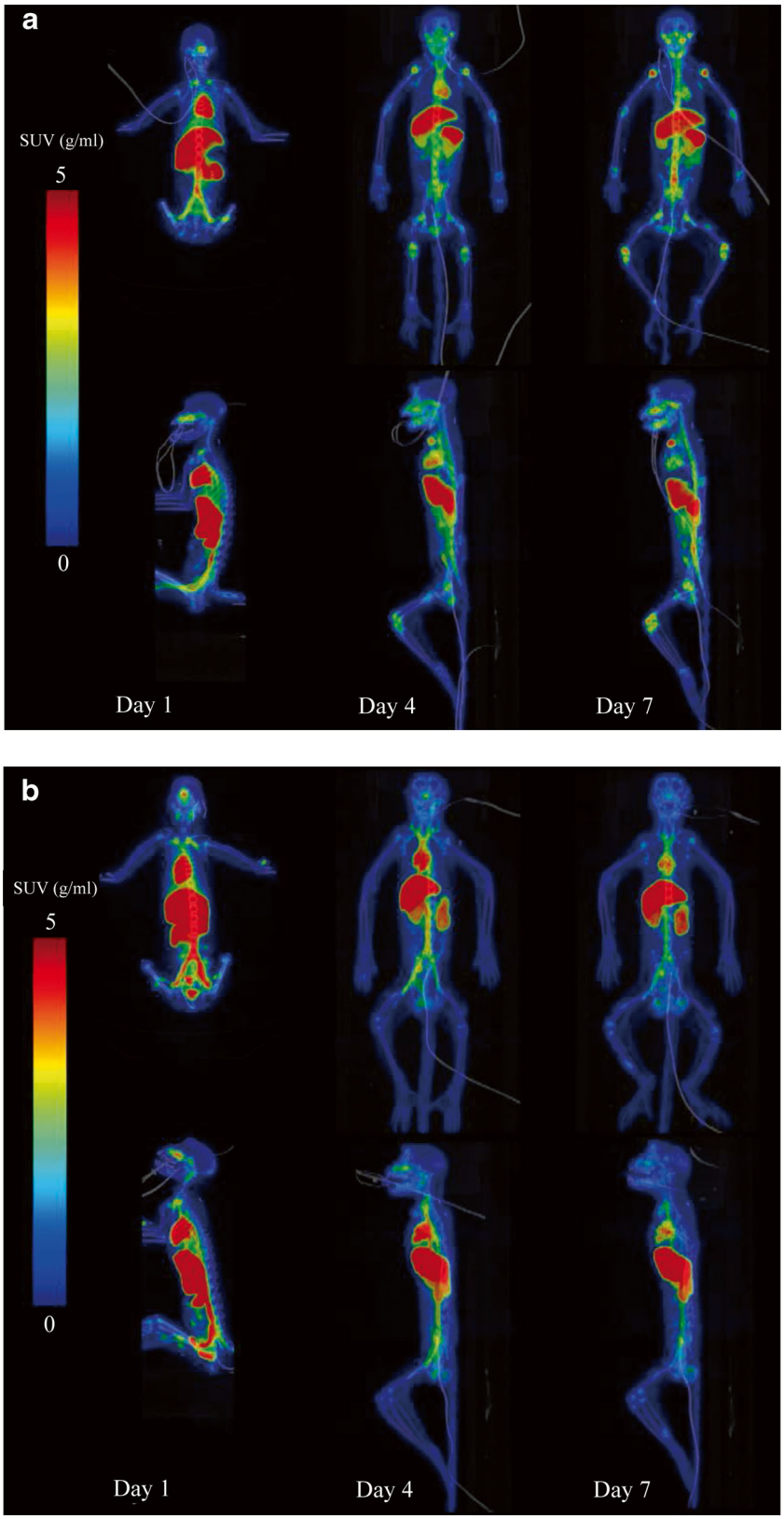

Fig. 1 Representative post dosing images of PET-CT scans for ^{89}Zr-KHK2866 and ^{89}Zr-KM8047. Post dosing images of PET-CT scans for ^{89}Zr-KHK2866 (**a**) ^{89}Zr-KM8047 (**b**) at a dose of 0.1 mg/kg on Days 1 (2 h post dosing), 4 (72 h), and 7 (144 h).

same kinetic observed for the blood pool. At 0.1 and 1 mg/kg, the splenic uptake stayed relatively high and constant over the 7 days, while at 10 mg/kg the kinetic was similar to the one observed in the other organs. Finally, the shoulder joints were

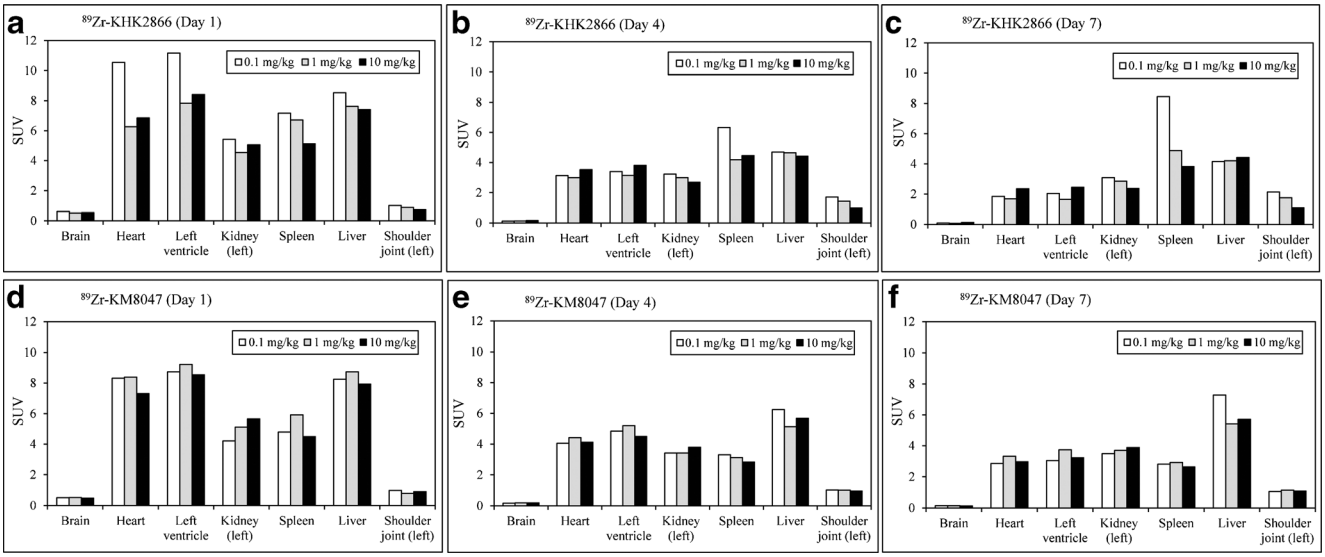

Fig. 2 Comparison of uptake profiles of ^{89}Zr-KHK2866 and ^{89}Zr-KM8047. The biodistribution of ^{89}Zr-KHK2866 (**a**-**c**) and ^{89}Zr-KM8047 (**d**-**f**) at doses of 0.1, 1, and 10 mg/kg on Days 1 (2 h post dosing), 4 (72 h), and 7 (144 h).

the only VOI in which the SUV increased over the time. A displacement of the uptake in the shoulder joints was observed at simultaneous dosing of either 1 or 10 mg/kg of cold KHK2866.

PET-CT Imaging of ^{89}Zr-N-succinyl-desferrioxamine-KM8047

The biodistribution of ^{89}Zr-KM8047 was similar to that of ^{89}Zr-KHK2866 with the exception of a less pronounced uptake in the joints (Figs. 1b and 2d–f). As opposed to ^{89}Zr-KHK2866, no apparent uptake displacement in the shoulder joints by cold KM8047 was observed. The other kinetics were very similar to those observed in the ^{89}Zr-KHK2866 immuno-PET study except that the splenic uptake followed the same wash-out kinetic as the other organs.

Measurement of Whole Blood and Serum Radioactivity

One blood sample obtained prior to dosing and seven blood samples obtained approximately 2, 4, 6, 24, 48, 72, and 144 h post dosing were used to measure the radioactivity in whole blood and serum in both phase 1 and 2 studies. Time activity curves for whole blood and serum expressed in SUV are shown in Fig. 3.

The maximum radioactivities of ^{89}Zr-KHK2866 were almost the same with those of ^{89}Zr-KM8047 for both whole blood and serum. On the other hand, more rapid decrease in radioactivities of ^{89}Zr-KHK2866 was observed compared to the time-radioactivity curves of ^{89}Zr-KM8047. In the time curves of ^{89}Zr-KHK2866, 10 mg/kg groups showed less rapid decrease in radioactivities than the other groups for both whole blood and serum.

PK Analysis

Serum concentrations of ^{89}Zr-KHK2866 and ^{89}Zr-KM8047 after single intravenous administration at doses of 0.1, 1, and 10 mg/kg to female cynomolgus monkeys were determined by an electrochemiluminescence assay (Fig. 4). Pharmacokinetic parameters of ^{89}Zr-KHK2866 and ^{89}Zr-KM8047 in serum are shown in Table I.

Serum concentration-time profiles of ^{89}Zr-KHK2866 and ^{89}Zr-KM8047 were similar up to 2 or 3 days after the administration in 0.1 and 1 mg/kg dose groups or 10 mg/kg groups, respectively. However, ^{89}Zr-KHK2866 serum concentrations from those time points afterwards were apparently lower than ^{89}Zr-KM8047 concentrations. The elimination half-life ($t_{1/2}$) and the total clearance (CL) values of ^{89}Zr-KHK2866 were shorter and larger than those of ^{89}Zr-KM8047, respectively. The area under the concentration-time curve (AUC) from zero to the time of the last measurable concentration ($AUC_{0\text{-}t}$) and the AUC from time 0 to infinity ($AUC_{0\text{-}\infty}$) values of ^{89}Zr-KHK2866 were smaller than those of ^{89}Zr-KM8047.

Evaluation of Serum and CSF Pharmacokinetics Following a Single Intravenous Dose of KHK2866 and KM8047 in Cynomolgus Monkeys

Serum concentration-time profiles of KHK2866 and KM8047 after single intravenous administration at doses of 1, 10, and 100 mg/kg to female cynomolgus monkeys are shown in Fig. 5a, and CSF concentration-time profiles of KHK2866 and KM8047 are shown in Fig. 5b. Pharmacokinetic parameters of KHK2866 and KM8047 in serum and CSF are shown in Tables II and III, respectively.

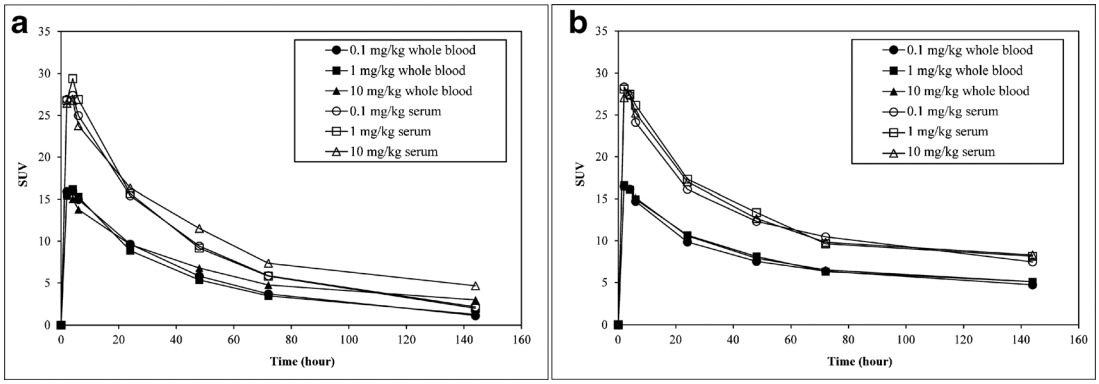

Fig. 3 Time-radioactivity curves of whole blood and serum when dosing of ^{89}Zr-KHK2866 and ^{89}Zr-KM8047. Time-radioactivity profiles of ^{89}Zr-KHK2866 (**a**) and ^{89}Zr-KM8047 (**b**). Whole and serum obtained pre-dosing and 2, 4, 6, 24, 48, 72, and 144 h post dosing were used to measure the radioactivity.

Serum concentrations of KHK2866 and KM8047 decreased biphasically after intravenous administration. Serum concentration-time profiles of KHK2866 and KM8047 up to 2 days after the administration were similar in each dose group, however, KHK2866 serum concentrations from 2 days onward after the administration were apparently lower than KM8047 concentrations, especially in the lower dose group. The $t_{1/2}$ and CL values of KHK2866 were shorter and larger than those of KM8047, respectively. The increase in the $AUC_{0\text{-}t}$ and $AUC_{0\text{-}\infty}$ values of KHK2866 was more than dose proportional.

CSF concentration-time profiles of KHK2866 and KM8047 after the intravenous administration showed obvious inter-individual variability in all dose groups. The maximum concentration (C_{max}) values and the $AUC_{0\text{-}t}$ values of KHK2866 and KM8047 increased with the increment of the dose level. Overall, there were no apparent differences in CSF concentrations and pharmacokinetic parameters between KHK2866 and KM8047.

The CSF-to-serum concentration ratios increased up to about 6 h after administration and then reached the plateau (data not shown). The CSF-to-serum concentration ratios of KHK2866 from 6 to 168 h after administration ranged from 0.00172 to 0.0393 (mean, $n=2$ in each dose group), and those of KM8047 ranged from 0.00168 to 0.0112, at a dose range of 1 to 100 mg/kg. There was inter-individual variability in CSF-to-serum concentration ratios in all dose groups and sampling time points. Both KHK2866 and KM8047 showed low central nervous system penetration and no marked differences between KHK2866 and KM8047 were observed.

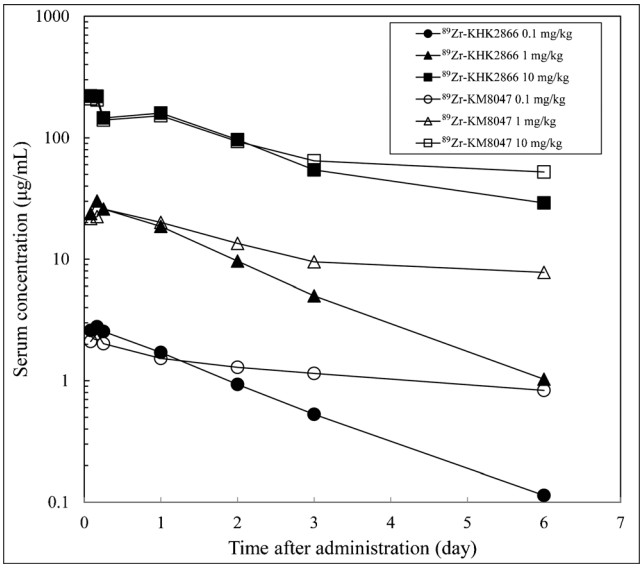

Fig. 4 Individual serum concentration-time profiles of ^{89}Zr-KHK2866 and ^{89}Zr-KM8047 after single intravenous administration at doses of 0.1, 1, and 10 mg/kg to female cynomolgus monkeys. Serum concentrations of decayed ^{89}Zr-KHK2866 and ^{89}Zr-KM8047 were measured by an electrochemiluminescence assay for the determination of human IgG in monkey serum. Serum samples obtained pre-dosing and 2, 4, 6, 24, 48, 72, and 144 h post dosing were used to measure the concentrations.

DISCUSSION

Epidermal growth factor (EGF) receptors and EGF family members represent promising targets for cancer therapy. Heparin-binding EGF-like growth factor (HB-EGF) is a member of the EGF family and is an important therapeutic target in some types of human cancers. The phase I study of KHK2866, a humanized anti-HB-EGF monoclonal antibody, was discontinued due to unacceptable neuropsychiatric toxicity observed at doses of 0.1, 1, and 3 mg/kg (4). Preclinical toxicology studies using cynomolgus monkeys have not been able to predict human neuropsychiatric adverse effects. Taking these results into account, we performed the reverse translational research in order to see whether we could observe noticeable distribution of KHK2866 to brain using cynomolgus monkeys.

First, the whole body biodistribution of ^{89}Zr-KHK2866 and ^{89}Zr-KM8047 was investigated using *in vivo* PET-CT imaging until 7 days post administration. The biodistribution of ^{89}Zr-KHK2866 was similar for the 3 doses (0.1, 1 and 10 mg/kg) (Figs. 1a and 2a-c). The MIP showed that ^{89}Zr-

Table I Pharmacokinetic Parameters of ^{89}Zr-KHK2866 and ^{89}Zr-KM8047 After Single Administration at Doses of 0.1, 1, and 10 mg/kg to Female Cynomolgus Monkeys

Test substance	Dose (mg/kg)	$t_{1/2}$ (day)	C_{max} (μg/ml)	AUC_{0-t} (μg·day/ml)	$AUC_{0-\infty}$ (μg·day/ml)	CL (ml/day/kg)	V_{ss} (ml/kg)
^{89}Zr-KHK2866	0.1	1.33	2.79	5.27	5.49	18.2	31.8
	1	1.26	30.2	53.7	55.6	18.0	30.0
	10	2.48	220	496	596	16.8	53.5
^{89}Zr-KM8047	0.1	6.35	2.45	7.49	15.1	6.62	58.7
	1	5.69	25.9	77.1	139	7.20	54.6
	10	5.43	210	536	932	10.7	76.8

PK parameters were obtained by non-compartmental analysis

KHK2866 accumulated in the liver, spleen and joints. The shoulder joints were the only VOI in which the SUV increased over the time. Furthermore, a displacement of the uptake in the shoulder joints was observed at simultaneous dosing of either 1 or 10 mg/kg of cold KHK2866, indicating specific distribution to shoulder joints of ^{89}Zr-KHK2866. No significant distribution of ^{89}Zr-KHK2866 to brain was detected. On the other hand, the biodistribution of ^{89}Zr-KM8047 was similar to that of ^{89}Zr-KHK2866 with the exception of a less pronounced uptake in the joints (Figs. 1b and 2d-f). Time-radioactivity curves of whole blood and serum showed that more rapid decrease in radioactivities of ^{89}Zr-KHK2866 was observed compared to the time-radioactivity curves of ^{89}Zr-KM8047 although the maximum radioactivities of those radiolabeled antibodies were almost the same for both whole blood and serum (Fig. 3). In the time-radioactivity curves of ^{89}Zr-KHK2866, 10 mg/kg groups showed less rapid decrease in radioactivities than the other groups for both whole blood and serum, suggesting saturation of antigen-dependent clearance at simultaneous dosing of 10 mg/kg of cold KHK2866. Antigen-dependent clearance of KM3566, a parental murine monoclonal antibody, was demonstrated by *in vitro* and *in vivo* experiments in our previous research (10). In addition, more rapid decrease in radioactivities of ^{89}Zr-KHK2866 as compared to ^{89}Zr-KM8047 was consistent with the results of serum concentration-time profiles of those radiolabeled antibodies (Fig. 4 and Table I).

Furthermore, as a separate study, KHK2866 and KM8047 concentrations in serum and cerebrospinal fluid were determined after administration of a single dose to obtain more supportive evidence. Serum concentrations of KHK2866 and KM8047 decreased biphasically after intravenous administration at doses of 1, 10, and 100 mg/kg to cynomolgus monkeys (Fig. 5a). The $t_{1/2}$ and CL values of KHK2866 were shorter and larger than those of KM8047, respectively (Table II). The increase in AUC_{0-t} and $AUC_{0-\infty}$ values of KHK2866 was more than dose proportional (Table II), suggesting the saturation of antigen-dependent clearance at higher dose ranges as discussed above. CSF concentration-time profiles of KHK2866 and KM8047 are shown in Fig. 5b. The C_{max} values and the AUC_{0-t} values of KHK2866 and KM8047 increased with the increment of the dose level (Table III). Overall, there were no apparent differences in CSF concentrations and pharmacokinetic parameters between KHK2866 and KM8047 (Table III). The CSF-to-serum concentration ratios increased up to about 6 h after

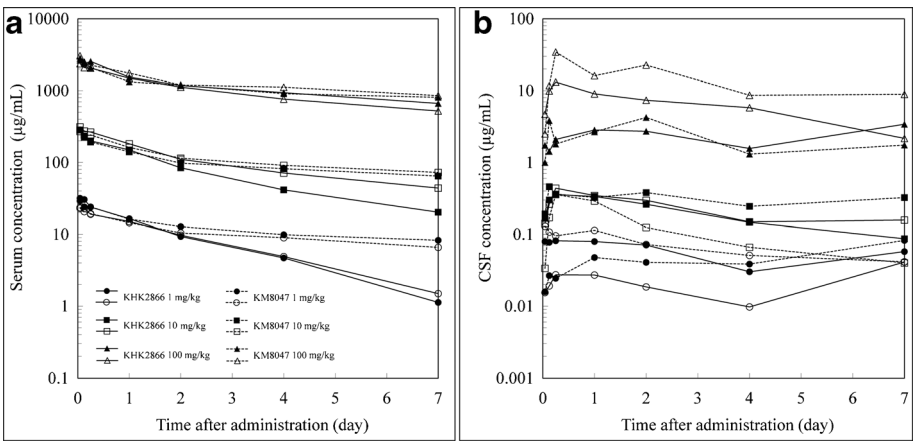

Fig. 5 Individual serum and CSF concentration-time profiles of KHK2866 and KM8047 after single intravenous administration at doses of 1, 10, and 100 mg/kg to female cynomolgus monkeys. Serum concentration-time profiles of KHK2866 and KM8047 (**a**) and CSF concentration-time profiles of KHK2866 and KM8047 (**b**). Serum and CSF samples obtained pre-dosing and 1, 3, 6, 24, 48, 96, and 168 h post dosing were used to measure the concentrations. Symbols and curves are common in (**a**) and (**b**).

Table II Pharmacokinetic Parameters of KHK2866 and KM8047 in Serum After Single Intravenous Administration at Doses of 1, 10, and 100 mg/kg to Female Cynomolgus Monkeys

Test substance	Dose (mg/kg)		$t_{1/2}$ (day)	C_{max} (μg/ml)	AUC_{0-t} (μg·day/ml)	$AUC_{0-\infty}$ (μg·day/ml)	CL (ml/day/kg)	V_{ss} (ml/kg)
KHK2866	1	1	1.62	31.7	58.2	61.0	16.4	35.1
		2	1.84	23.5	55.0	59.1	16.9	42.7
		Mean	1.73	27.6	56.6	60.1	16.7	38.9
	10	1	2.47	285	528	598	16.7	49.6
		2	3.79	314	742	979	10.2	48.6
		Mean	3.13	300	635	789	13.5	49.1
	100	1	6.07	2650	8060	13900	7.19	58.9
		2	4.60	2370	7000	10400	9.62	59.5
		Mean	5.34	2510	7530	12200	8.41	59.2
KM8047	1	1	8.23	29.2	86.3	183	5.47	61.7
		2	7.39	23.1	73.5	145	6.92	69.9
		Mean	7.81	26.2	79.9	164	6.20	65.8
	10	1	8.31	284	705	1480	6.77	76.1
		2	7.66	272	806	1600	6.25	64.6
		Mean	7.99	278	756	1540	6.51	70.4
	100	1	9.37	2810	7850	18500	5.41	70.5
		2	10.0	3060	8930	21500	4.65	63.8
		Mean	9.69	2940	8390	20000	5.03	67.2

The pharmacokinetic parameters were calculated from the serum concentrations of KHK2866 or KM8047 for 7 days after the administration

administration and then reached the plateau. The ratios of KHK2866 from 6 to 168 h after administration ranged from 0.00172 to 0.0393 at a dose range of 1 to 100 mg/kg while those of KM8047 ranged from ranged from 0.00168 to

Table III Pharmacokinetic Parameters of KHK2866 and KM8047 in CSF After Single Intravenous Administration at Doses of 1, 10, and 100 mg/kg to Female Cynomolgus Monkeys

Test substance	Dose (mg/kg)		C_{max} (μg/ml)	AUC_{0-t} (μg·day/ml)
KHK2866	1	1	0.0820	0.388
		2[a]	0.0413	0.153
		Mean	0.0617	0.271
	10	1	0.357	1.38
		2	0.439	1.59
		Mean	0.398	1.49
	100	1[a]	3.42	16.8
		2	13.2	43.8
		Mean	8.31	30.3
KM8047	1	1[a]	0.0829	0.339
		2	0.130	0.460
		Mean	0.106	0.400
	10	1	0.460	2.18
		2	0.358	0.845
		Mean	0.409	1.51
	100	1	4.25	15.9
		2	34.5	99.6
		Mean	19.4	57.8

The pharmacokinetic parameters were calculated from the CSF concentrations of KHK2866 or KM8047 for 7 days after the administration

[a] The pharmacokinetic parameters were calculated from the CSF concentrations of KHK2866 or KM8047 for 4 days after the administration expect for the last sampling point (168 h)

0.0112 at the same dose range. It is usually assumed that antibodies cannot cross the blood–brain barrier (BBB) unless there is a specific transport system for them at the BBB. In general, antibody penetration into brain (CSF/serum ratio) has been reported to be >0.1% in animal models and in human patients (11–14). The CSF/serum ratios for KHK2866 and KM8047 showed similar values with those reported for other antibodies, indicating no significant BBB penetration for both antibodies. Furthermore, it is of note that no marked differences between the two antibodies were observed.

A previous study indicates that HB-EGF is expressed in normal human tissues like lung, liver, kidney, pancreas, brain, and ovary (15). Moreover, HB-EGF distribution pattern of normal human tissues is similar to that of normal cynomolgus monkey tissues based on our internal study (data not shown). Given that there are many reports that HB-EGF mRNA and protein are widely expressed in rodent brain (16–19), HB-EGF may play an important function also in human and non-human primates.

There is a possible mechanism for neuropsychiatric toxicity of anti-HB-EGF antibody even with its normal distribution to brain. HB-EGF is synthesized as a membrane-anchored protein (proHB-EGF), composed of a signal peptide, propeptide, heparin-binding, EGF-like, juxtamembrane, transmembrane, and cytoplasmic domains (20). ProHB-EGF is cleaved at its juxtamembrane domain by metalloproteases in a process called ectodomain shedding, yielding a soluble form of HB-EGF (21). In clinical phase I study, serum soluble free HB-EGF levels were measured by the previously developed method (22). As a result, all KHK2866 doses from 0.1 to 3 mg/kg decreased serum free HB-EGF levels, generally below the lower limit of quantitation. CSF soluble HB-EGF might be decreased due to break of CSF/blood equilibrium or *in situ* neutralization by KHK2866, although we have not measured its concentrations.

CONCLUSION

In summary, PET studies with monkeys revealed ^{89}Zr-KHK2866 accumulation in the liver, spleen and joints of multiple parts, but not in the brain. In addition, the pharmacokinetic analyses in serum and CSF demonstrated a low penetration of KHK2866 into the brain. These studies indicate the difficulty of prediction for neuropsychiatric toxicity of monoclonal antibodies in human by means of pharmacokinetic evaluations using cynomolgus monkeys.

ACKNOWLEDGMENTS AND DISCLOSURES

We thank Drs. T. Tawara, N. Mimura, A. Takami, Y Yoda, J Hosogi, K Fujita, H. Kaito, and TW. Poh for excellent support and helpful suggestion. This research was funded by Kyowa Hakko Kirin, Co. Ltd.

REFERENCES

1. Higashiyama S, Iwabuki H, Morimoto C, Heida M, Inoue H, Matsushita N. Membrane-anchored growth factors, the epidermal growth factor family: beyond receptor ligands. Cancer Sci. 2008;99:214–20.
2. Yotsumoto F, Yagi H, Suzuki SO, Oki E, Tsujioka H, Hachisuga T, *et al.* Validation of HB-EGF and amphiregulin as targets for human cancer therapy. Biochem Biophys Res Commun. 2008;365:555–61.
3. Miyamoto S, Iwamoto R, Furuya A, Takahashi K, Sasaki Y, Ando H, *et al.* A novel anti-human HB-EGF monoclonal antibody with multiple antitumor mechanisms against ovarian cancer cells. Clin Cancer Res. 2011;17:6733–41.
4. Sarantopolous J, Camacho L, Mita M, Cranmer L, Birrer M, Bristow P, Kaito H, Strout V. Phase I study of monotherapy with KHK2866, an anti-heparin-binding epidermal growth factor-like growth factor monoclonal antibody, in patients with advanced cancer. Target Oncol. In press.
5. Rahmim A, Zaidi H. PET versus SPECT: strengths, limitations and challenges. Nucl Med Commun. 2008;29:193–207.
6. Börjesson PK, Jauw YW, Boellaard R, de Bree R, Comans EF, Roos JC, *et al.* Performance of immuno-positron emission tomography with zirconium-89-labeled chimeric monoclonal antibody U36 in the detection of lymph node metastases in head and neck cancer patients. Clin Cancer Res. 2006;12:2133–40.
7. Dijkers EC, Oude Munnink TH, Kosterink JG, Brouwers AH, Jager PL, de Jong JR, *et al.* Biodistribution of 89Zr-trastuzumab and PET imaging of HER2-positive lesions in patients with metastatic breast cancer. Clin Pharmacol Ther. 2010;87:586–92.
8. Vugts DJ, Heuveling DA, Stigter-van Walsum M, Weigand S, Bergstrom M, van Dongen GA, *et al.* Preclinical evaluation of 89Zr-labeled anti-CD44 monoclonal antibody RG7356 in mice and cynomolgus monkeys: prelude to phase 1 clinical studies. MAbs. 2014;6(2):567–75.
9. Verel I, Visser GW, Boellaard R, Stigter-van Walsum M, Snow GB, van Dongen GA. ^{89}Zr immuno-PET: comprehensive procedures for the production of ^{89}Zr-labeled monoclonal antibodies. J Nucl Med. 2003;44:1271–81.
10. Kasai N, Yoshikawa Y, Enokizono J. Effect of antigen-dependent clearance on pharmacokinetics of anti-heparin-binding EGF-like growth factor (HB-EGF) monoclonal antibody. MAbs. 2014;6(5):1220–8.
11. Pardridge WM. Drug targeting to the brain. Pharm Res. 2007;24(9):1733–44.
12. Rubenstein JL, Combs D, Rosenberg J, Levy A, McDermott M, Damon L, *et al.* Rituximab therapy for CNS lymphomas: targeting the leptomeningeal compartment. Blood. 2003;101(2):466–8.
13. Poduslo JF, Curran GL, Berg CT. Macromolecular permeability across the blood-nerve and blood–brain barriers. Proc Natl Acad Sci U S A. 1994;91:5705–9.
14. Petereit HF, Rubbert-Roth A. Rituximab levels in cerebrospinal fluid of patients with neurological autoimmune disorders. Mult Scler. 2009;15(2):189–92.
15. Nakamura Y, Handa K, Iwamoto R, Tsukamoto T, Takahasi M, Mekada E. Immunohistochemical distribution of CD9, heparin binding epidermal growth factor-like growth factor, and integrin alpha3beta1 in normal human tissues. J Histochem Cytochem. 2001;49:439–44.

16. Hayase Y, Higashiyama S, Sasahara M, Amano S, Nakagawa T, Taniguchi N, *et al.* Expression of heparin-binding epidermal growth factor-like growth factor in rat brain. Brain Res. 1998;784(1–2): 163–78.
17. Abraham JA, Damm D, Bajardi A, Miller J, Klagsbrun M, Ezekowitz RA. Heparin-binding EGF-like growth factor: characterization of rat and mouse cDNA clones, protein domain conservation across species, and transcript expression in tissues. Biochem Biophys Res Commun. 1993;190(1):125–33.
18. Mishima K, Higashiyama S, Nagashima Y, Miyagi Y, Tamura A, Kawahara N, *et al.* Regional distribution of heparin-binding epidermal growth factor-like growth factor mRNA and protein in adult rat forebrain. Neurosci Lett. 1996;213:153–6.
19. Nakagawa T, Sasahara M, Hayase Y, Haneda M, Yasuda H, Kikkawa R, *et al.* Neuronal and glial expression of heparin-binding EGF-like growth factor in central nervous system of prenatal and early postnatal rat. Brain Res Dev Brain Res. 1998;108:263–72.
20. Higashiyama S, Lau K, Besner GE, Abraham JA, Klagsbrun M. Structure of heparin-binding EGF-like growth factor. Multiple forms, primary structure, and glycosylation of the mature protein. J Biol Chem. 1992;267(19):6205–12.
21. Goishi K, Higashiyama S, Klagsbrun M, Nakano N, Umata T, Ishikawa M, *et al.* Phorbol ester induces the rapid processing of cell surface heparin-binding EGF-like growth factor: conversion from juxtacrine to paracrine growth factor activity. Mol Biol Cell. 1995;6:967–80.
22. Kasai N, Kobayashi K, Shioya S, Yoshikawa Y, Yotsumoto F, Miyamoto S, *et al.* Soluble heparin-binding EGF-like growth factor (HB-EGF) detected by newly developed immuno-PCR method is a clear-cut serological biomarker for ovarian cancer. Am J Transl Res. 2012;4:415–21.